Int. J. Electrochem. Sci., 11 **(2016)** 6204 – 6214, doi: 10.20964/2016.07.69

International Journal of ELECTROCHEMICAL SCIENCE
www.electrochemsci.org

Binary Cobalt and Magnesium Hydroxide Catalyst for Oxygen Evolution Reaction in Alkaline Water Electrolysis

Imgon Hwang[1], *Injoon Jang*[1], *Gibaek Lee*[1,2] *and Yongsug Tak*[1,*]

[1] Department of Chemical Engineering, Inha University, 253 Yonghyun-dong, Nam-ku, Incheon 402-751, Republic of Korea
[2] Department of Physics, Martin-Luther University of Halle-Wittenberg, Halle (Saale) 06099, Germany
[*]E-mail: ystak@inha.ac.kr

Received: 24 March 2016 / *Accepted:* 14 May 2016 / *Published:* 4 June 2016

Alkaline water electrolysis has been proposed as an environmentally inoffensive way to supply the anticipated demand for hydrogen gas (H_2) for the prospective hydrogen energy economy. However, in practice, the efficiency of water electrolysis is limited by the large anodic overpotential of the oxygen evolution reaction (OER). Therefore, the development of catalysts having a low overpotential and high activity is required in order to reduce the cost and improve the efficiency of the alkaline OER. Herein, we focused on decreasing the overpotential and increasing the catalyst activity by simultaneous use of synthesized carbon-supported cobalt oxide and magnesium oxide as an electrochemical catalyst for the alkaline OER. The activity of the carbon-supported cobalt and magnesium hydroxide, $Co(OH)_2$-$Mg(OH)_2$/C, catalyst was dependent on the pH and metal composition ratio. The highest activity and lowest overpotential were achieved with the catalyst having a $Co(OH)_2$ to $Mg(OH)_2$ ratio of 84:16 prepared at pH 9.5.

Keywords: $Mg(OH)_2$, $Co(OH)_2$, Oxygen evolution reaction, Alkaline water electrolysis, Carbon

1. INTRODUCTION

Increasing concerns about global warming and energy conversion have continued to drive the search for renewable energy sources and energy storage technologies as alternatives to fossil-fuel-based technology [1-4]. Hydrogen is regarded as the future energy source based on its high energy capacity and heat of combustion as compared to that of fossil-fuel sources [5-8]. Hydrogen for power can be produced at low cost via alkaline water electrolysis via several processes with the added advantages of water utilization efficiency and safety. The following equations correspond to the

electrochemical reactions that occur at the cathode and anode during this process under alkaline conditions:

The hydrogen evolution reaction (HER) at the cathode:

$$2H_2O + 2e^- \rightarrow H_2 + 2OH^- \quad (1)$$

The oxygen evolution reaction (OER) at the anode:

$$4OH^- \rightarrow O_2 + 2H_2O + 4e^- \quad (2)$$

The development of more stable catalysts with high catalytic activity and low overpotential as anode catalysts for the alkaline water electrolysis is particularly important because the OER process has a large overpotential, which leads to deterioration of the performance of the water electrolysis system.

Extensive research has been undertaken for the development of anode catalysts for alkaline water electrolysis. Noble-metals, such as Ru and Ir, exhibit high activity in the OER. However, the high cost of these materials and their low stability in alkaline conditions limit their application, although the catalyst activity can be enhanced by inclusion of Ta. The use of transition metals with high stability and activity under alkaline conditions, such as Ni, Co, Fe and Mn [9-11], has been evaluated in many studies to enhance the catalyst activity for the alkaline oxygen evolution reaction because the high oxidation state of these metals is advantageous for promoting the OER activity. Furthermore, in order to enhance the catalyst activity and reduce the overpotential, two transition metals have been combined in many studies. Cobalt-based metal catalysts have been reported to be good electrocatalysts for the alkaline OER [12-14]; these include Co-Ni [15], Co-Fe [16], and Co-Mn [17] that reportedly have very high electrochemical activity for the OER.

Several methods for preparing cobalt-based (hydr)oxide catalysts have been developed, including thermal decomposition [18], sol-gel [19], precipitation [20], electrospinning [21], gel hydrothermal oxidation [22], electrodeposition [23,24], and the polyol method [25]. The catalytic activity of the catalysts prepared by these methods is significantly influenced by the concentration and condition of the metal salt precursors [9].

In this study, we introduce for the first time, a catalyst comprising magnesium hydroxide combined with cobalt hydroxide on a carbon support prepared via a modified polyol method that exhibits excellent conductivity with high distribution of the catalyst material on the support. Magnesium has not previously been studied for alkaline water electrolysis, although magnesium is known as an excellent metal for the anode in air battery applications due to its high theoretical specific charge capacity [26-27]. The modified polyol method is also a well-known process that has been used to generate monodisperse and well-distributed metal powders, including a redox reaction metallic precursor with a liquid polyol [28-29]. Herein, we also investigate the physical properties and electrochemical activity of the $Co(OH)_2$-$Mg(OH)_2$ catalyst. The developed catalyst shows remarkable potential for the alkaline OER.

2. EXPERIMENTAL

2.1. Synthesis of carbon supported $Co(OH)_2$-$Mg(OH)_2$ catalyst

Bimetallic metal hydroxides were prepared by using a modified polyol method [30]. The metal precursors (anhydrous $CoCl_2$ and $MgCl_2 \cdot 4H_2O$) were separately dissolved in 50 mL ethylene glycol and subsequently combined. A homogeneous mixture was obtained via ultrasonic stirring. Vulcan XC-72 (500 mg; Cabot Corp., BET: 235 m^2g^{-1}, denoted as C) was suspended in 250 mL ethylene glycol and ultrasonicated to form a homogeneous mixture. The two-metal solution was combined with this mixture and the solution pH was adjusted to 9.5 using 1 M NaOH, followed by heating at 160°C for 3 h with stirring. The mixture was stirred for 24 h. Finally, the resulting product was centrifugally separated and dried in an oven at 110°C for 12 h. $Co(OH)_2$/C, $Mn(OH)_2$/C, and $Co(OH)_2$-$Mn(OH)_2$/C catalysts were also prepared by the same method.

2.2 Physical characterization

The crystallinity of the prepared catalysts was analyzed by X-ray diffraction (XRD, Rigaku, D/max-2200), and the weight of the carbon-supported metal hydroxides was confirmed via thermogravimetric analysis (TGA, PERKIN ELMER, TG/DTA 6300). The distribution of the carbon-supported metal hydroxides was examined through transmission electron microscopy (TEM, JEOL, JEOL-2100F) with EDX-mapping, and the metal ratios of the synthesized catalysts were investigated by using inductively coupled plasma optical emission spectroscopy (ICP-OES, PERKIN ELMER, Optima 7300DV).

2.3 Electrochemical measurements

Electrochemical characterizations for alkaline water electrolysis were carried out using a potentiostat (Autolab PGSTAT302N). The catalyst layer on the glassy carbon electrode (GCE, 0.071 cm^2) was prepared by the following procedure. A mixture containing water, catalyst, and Nafion solution was homogeneously stirred for 1 h in an ultrasonic bath. A 3 μL aliquot of the mixture solution was dropped onto the GCE surface (the catalyst loading was 0.03 mg/cm^2) and dried in air at room temperature. Pt foil and 1 M KOH solution were used as the counter electrode and electrolyte, respectively. The electrochemical properties for OER were investigated in the potential range of 0.0 to 1.0 V (vs. Ag/AgCl sat'd 4 M KCl) in a three electrode testing system, at 4000 rpm, using a scan rate of 20 mVs^{-1}. An alkaline electrolysis test was also performed at a current density of 50 $mAcm^{-2}$ for 5 min using a two-electrode system; Pt foil was used as the counter electrode and the metal hydroxide catalyst on the GCE was used as a working electrode, similar to the working electrode of the 3-electrode system.

3. RESULTS AND DISCUSSION

For the $Co(OH)_2$-$Mg(OH)_2$/C catalyst prepared by the modified polyol method, the electrostatic force between the metal precursors and the carbon support was significantly affected by the pH of the solution, leading to differences in the amount, crystallinity, and catalytic activity of the synthesized metal (hydr)oxides [31]. In order to determine the optimal pH for maximizing the catalyst activity for the oxygen evolution reaction in alkaline media, $Co(OH)_2$-$Mg(OH)_2$/C electrocatalysts were synthesized under various pH conditions.

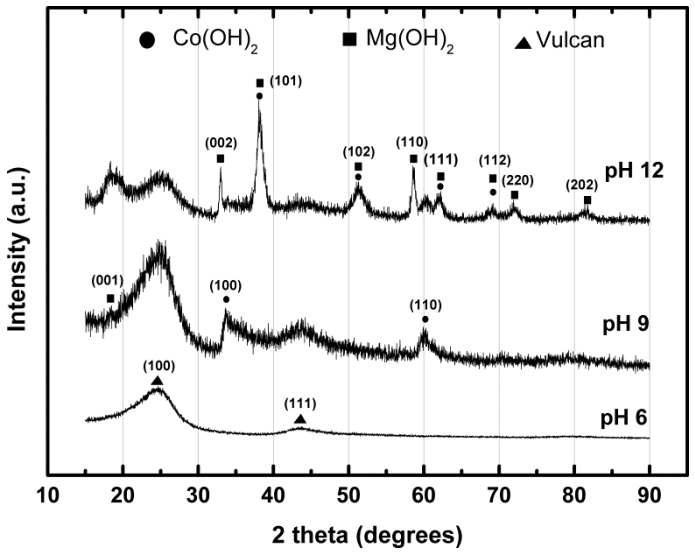

Figure 1. XRD patterns of $Co(OH)_2$-$Mg(OH)_2$/C catalysts prepared at pH 6, 9 and 12.

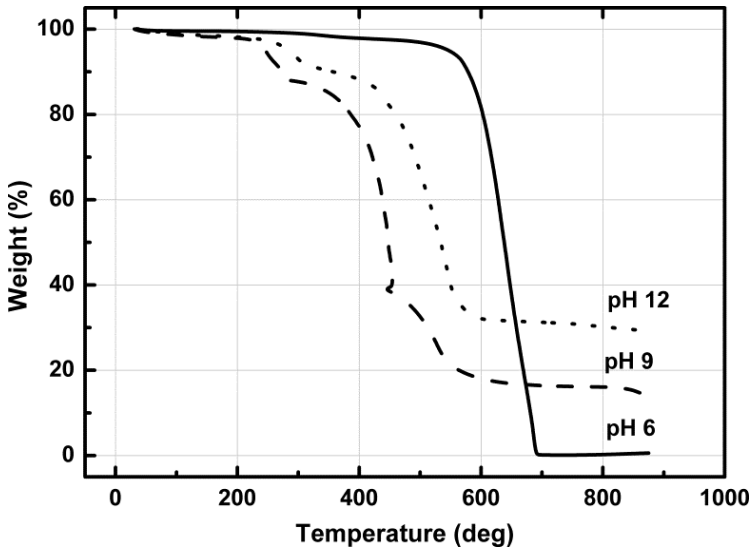

Figure 2. TGA of $Co(OH)_2$-$Mg(OH)_2$/C catalysts prepared at pH 6, 9 and 12. Temperature profile: 25°C – 900°C, 30°C/min in air environment.

Figure 1 shows the XRD patterns of the $Co(OH)_2$-$Mg(OH)_2$/C catalysts prepared at pH 6, 9, and 12. The crystallinity of the metal hydroxides increased as the pH increased. No crystalline phases of the cobalt (hydro)oxides and magnesium (hydro)oxides were detected at pH 6. As the pH increased to 9, both $Co(OH)_2$ and $Mg(OH)_2$ were formed and crystalline phases of $Mg(OH)_2$ and $Co(OH)_2$ were largely formed at pH 12.

Figure 2 indicates that the respective weight percentages of the $Co(OH)_2$ and $Mg(OH)_2$ catalysts prepared on the carbon support at pH 6, 9, and 12 were approximately 0.5, 14.2, and 29.1 wt.%, as confirmed by thermogravimetric analysis. A large amount of metal hydroxides was deposited on the carbon support as the pH of the synthesis mixture increased. The TGA curve for the specimen prepared at pH 9 indicated 3 distinct regions of weight loss for the catalyst with increasing temperature. After desorption of water, $Co(OH)_2$ was dehydrated to generate Co_3O_4 in the range of 220˚C to 280˚C. Subsequently, rapid weight loss occurred between 280˚C and 450˚C, which could be attributed to the decomposition of $Mg(OH)_2$ and crystallization of the MgO particles, combined with combustion of carbon [32]. Finally, the relatively slow weight reduction observed above 450˚C is attributed mainly to carbon combustion. For the specimen prepared at pH 12, the weight reduction occurred in two steps. The first step is the dehydration of cobalt hydroxides, followed by simultaneous decomposition of the magnesium hydroxides and carbon combustion in the second step. Carbon combustion was largely completed around 600°C.

Table 1. Cobalt and magnesium weight percentage in $Co(OH)_2$-$Mg(OH)_2$/C catalysts prepared under different pH conditions.

Sample	pH	Co (wt.%)	Mg (wt.%)
$Co(OH)_2$-$Mg(OH)_2$/C	6	-	-
	9	16.1	3.2
	9.5	16.9	4.6
	10	22.1	7.1
	12	21.7	11.5

The difference in the temperature ranges where the carbon support decomposes may be affected by the differences in the amount of cobalt in the samples. Cobalt acts as a catalyst that accelerates carbon oxidation. Therefore, as the content of cobalt increases, the temperature for carbon oxidation decreases [33]. The ratio of $Co(OH)_2$ relative to $Mg(OH)_2$ in the $Co(OH)_2$-$Mg(OH)_2$/C catalyst, determined via ICP-OES analysis, is shown in Table 1. Although the content of cobalt in the catalyst prepared at pH 12 was high, the amount of magnesium also increased concomitantly. It may be supposed that the effect of cobalt on carbon oxidation declined. However, the (hydro)oxide forms of cobalt and magnesium were not formed at relatively low pH 6. Ultimately, the catalyst prepared at pH 9 resulted in the lowest temperature for carbon oxidation.

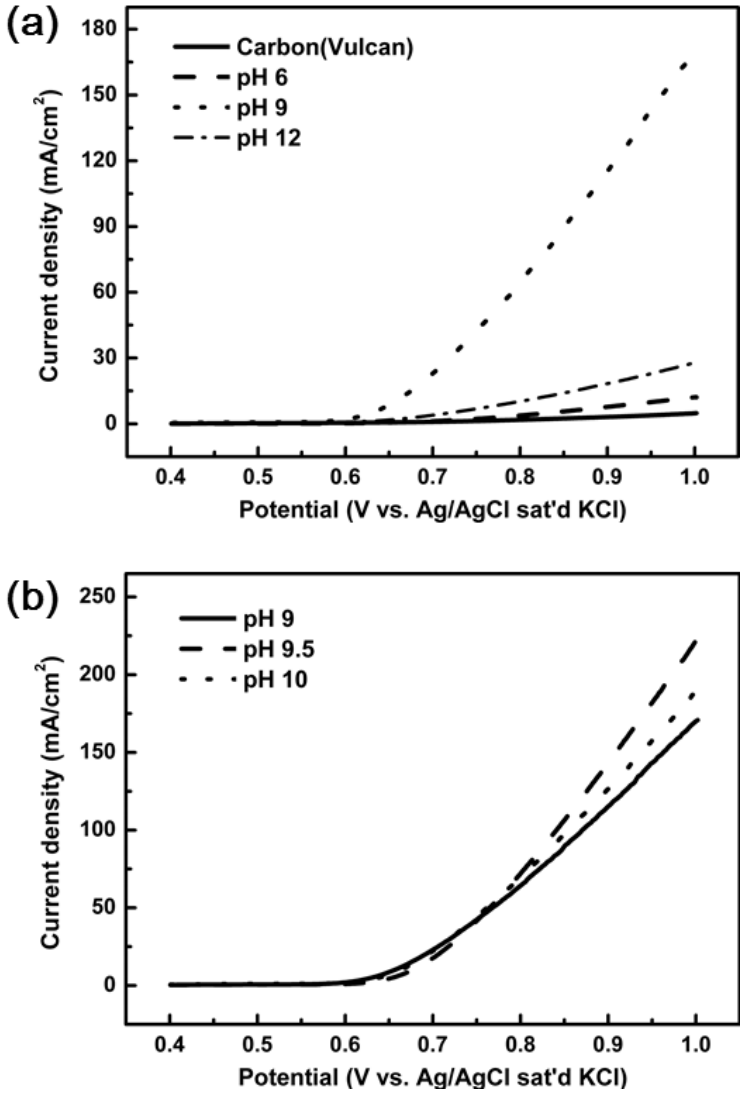

Figure 3. Anodic polarization curves of $Co(OH)_2$-$Mg(OH)_2$/C catalysts for oxygen evolution reaction; catalysts were prepared under different pH conditions: (a) pH 6, 9, 12 and (b) 9, 9.5, 10; data acquired in N_2-saturated 1 M KOH at scan rate of 20 mV/s.

Figure 3a shows the linear sweep voltammograms of the $Co(OH)_2$-$Mg(OH)_2$/C catalysts synthesized at pH 6, 9, and 12 compared with the pristine carbon electrode. The catalyst synthesized at pH 9 exhibited very high OER activity, whereas the catalysts synthesized at pH 6 and 12 exhibited relatively low OER activity. One possible reason is that the catalyst prepared at pH 12 has a higher $Mg(OH)_2$ content than the catalysts synthesized at pH 6 and 9, and $Mg(OH)_2$ may occupy the active sites of $Co(OH)_2$ for OER. For detailed analysis of the effect of the solution pH on the catalyst activity, the OER activity of each catalyst was measured at around pH 9 and compared (Fig. 3b). The results indicated that the activity of the $Co(OH)_2$-$Mg(OH)_2$/C catalyst synthesized at pH 9.5 was the highest among those of the three catalysts synthesized at different pH. The initiation potentials of the three catalysts showed similar values at around 0.6 V, whereas the catalysts exhibited different activities for the OER.

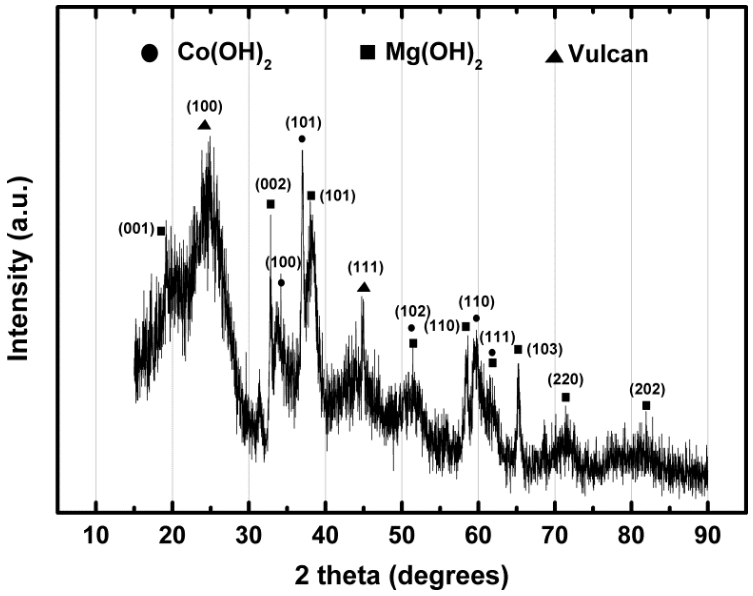

Figure 4. XRD patterns of $Co(OH)_2$-$Mg(OH)_2$/C catalysts prepared at pH 9.5.

The XRD patterns presented in Fig. 4 confirmed the presence of various lattice patterns for the $Co(OH)_2$-$Mg(OH)_2$/C catalyst synthesized at pH 9.5 and the high crystallinity of the sample. Thus, it could be inferred that the catalyst should enable a high degree of the oxygen evolution reaction for alkaline electrolysis. Although all of the synthesized catalysts are based on $Co(OH)_2$, the $Co(OH)_2$ to $Mg(OH)_2$ ratios of the catalysts varied depending on the pH used for synthesis, as shown in Table 1. The data suggest that $Mg(OH)_2$ does not affect the onset potential for the OER but contributes greatly to the catalyst activity. Thus, appropriate $Mg(OH)_2$ addition is considered to improve the OER activity.

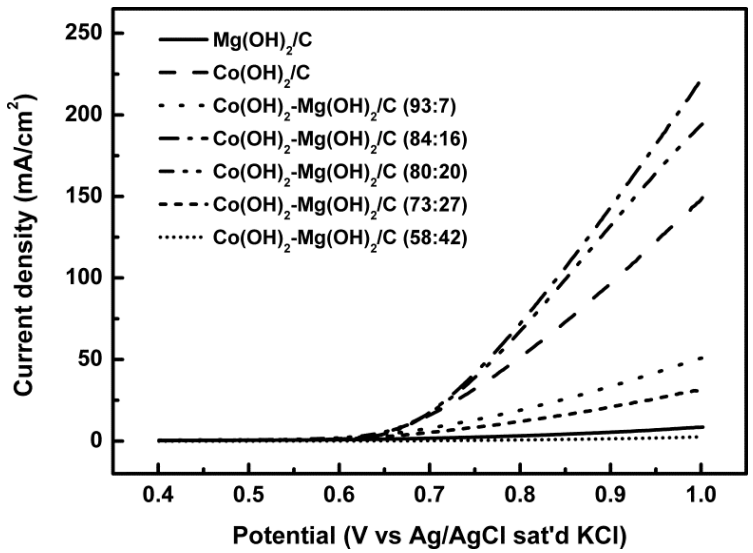

Figure 5. Anodic polarization curves acquired in N_2-saturated 1 M KOH at scan rate of 20 mV/s for $Co(OH)_2$-$Mg(OH)_2$/C catalysts with different Co/Mg ratios for oxygen evolution; catalysts were prepared at pH 9.5.

Based on the fact that the $Mg(OH)_2$ ratio has a significant impact on the catalyst activity, catalysts were synthesized by adjusting the amount of Mg while maintaining the pH of the synthesis solution at 9.5, where the highest activity for OER was achieved. The OER activities of the catalysts synthesized with different weight ratios of $Co(OH)_2$ to $Mg(OH)_2$ are shown in Fig. 5, where the ratios are the weight percentages of metal hydroxides only, analyzed via ICP-OES, and exclude the carbon support. The data in Fig. 5 confirmed that the addition of $Mg(OH)_2$ significantly enhanced the catalyst activity, although the $Co(OH)_2$/C catalyst itself exhibits high OER activity. The optimal $Co(OH)_2$ to $Mg(OH)_2$ ratio for maximizing the catalyst activity was 84:16, and a too low $Mg(OH)_2$ content (93:7) or too high $Mg(OH)_2$ content (73:27, 58:42) reduced the catalytic activity for the OER.

In OER kinetics, it is known that synergistic effects of the hydrous properties of individual hydroxides may operate, thereby accelerating formation of the $(OH)_2^-$ intermediates during the OER process when cobalt hydroxides coexist with other metal hydroxides on the surface of the catalyst [34]. On the other hand, if the bonding (Co-OH) between the active cobalt oxide sites and OH is very strong and stable, the turnover frequency of the oxygen evolution reactions becomes very low. Therefore, cobalt hydroxides act as a poison that reduces the OER activity on the catalyst surface [35]. If the appropriate ratio of $Mg(OH)_2$/C is combined with $Co(OH)_2$, the Co-OH bonding will be weakened to increase the overall OER activity.

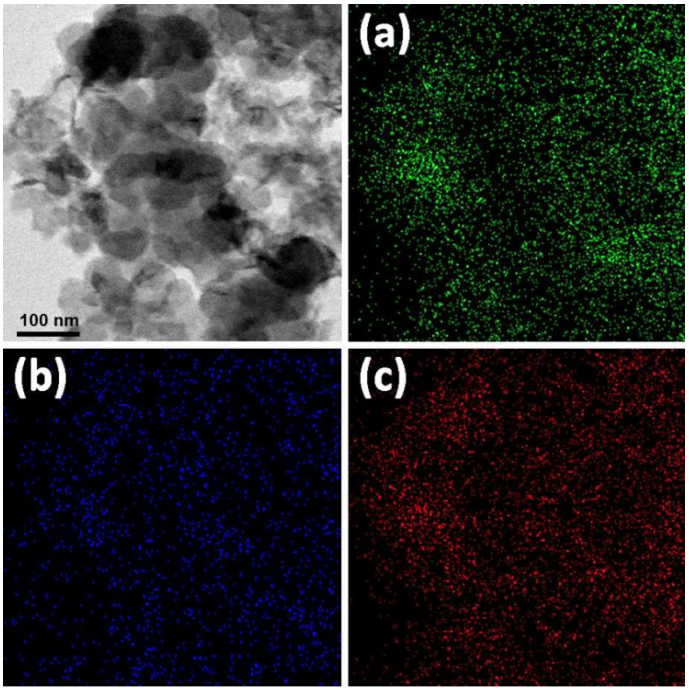

Figure 6. TEM image of $Co(OH)_2$-$Mg(OH)_2$/C (84:16 ratio) catalyst prepared at pH 9.5 showing where the elemental maps were obtained. Mappings of the elements (a) cobalt, (b) magnesium, and (c) oxygen elements.

Figure 6 shows the TEM image of the $Co(OH)_2$-$Mg(OH)_2$/C catalyst with a $Co(OH)_2$ to $Mg(OH)_2$ ratio of 84:16 synthesized at pH 9.5 where the highest OER activity was achieved. The image was analyzed using EDX-mapping in order to identify the individual elements. Cobalt is

indicated by green (Fig. 3a), magnesium by blue, (Fig. 3b), and oxygen by red (Fig. 3c). Uniform distribution of each element without agglomeration on one side was confirmed, though the particles were very small.

The $Co(OH)_2$-$Mg(OH)_2$/C catalyst was compared with other catalysts reported to have excellent activity [36] by synthesizing several single metal oxides and bimetallic oxide catalysts using the same method.

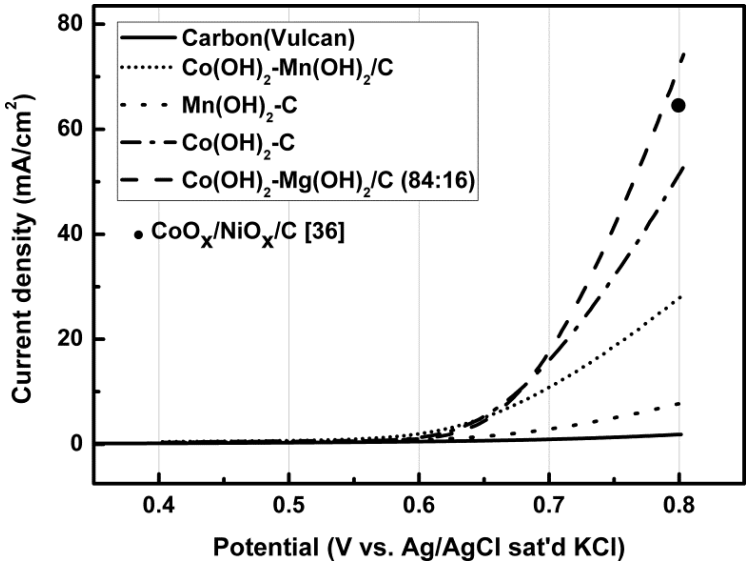

Figure 7. Comparison of anodic polarization curves acquired in N_2-saturated 1 M KOH at scan rate of 20 mV/s for single metal oxide and bimetallic oxide catalysts for oxygen evolution; catalysts were prepared at pH 9.5.

Figure 7 shows that the $Co(OH)_2$-$Mg(OH)_2$/C catalyst exhibited higher OER activity than the individual synthesized catalysts and the pristine carbon electrode. In particular, the $Co(OH)_2$-$Mg(OH)_2$/C catalyst exhibited higher OER activity than the $Co(OH)_2$-$Ni(OH)_2$/C catalyst (Fig. 7; black dot [36]) which is known for its very high OER activity. In addition, the $Co(OH)_2$-$Mg(OH)_2$/C catalyst had a higher exchange current density (1.37×10^{-3} A/cm^2) than the $Co(OH)_2$-$Ni(OH)_2$/C catalyst (1.74×10^{-4} A/cm^2) [37], as calculated from the Tafel plot:

$$\log i_{net} = \log i_o + (1-\alpha)n\mathrm{F}\eta/2.303\mathrm{RT} \quad (3)$$

where i_{net} is the current density, i_o is the exchange current density, n is the number of electrons included in the reactions, F is the Faraday constant, η is the overpotential, and R is the gas constant, T is the temperature, and α is the anodic transfer coefficient.

The as-prepared catalysts were applied to actual alkaline water electrolysis at a current density of 50 mA/cm^2 using a Pt cathode. Figure 8 shows that the $Co(OH)_2$-$Mg(OH)_2$/C catalyst had the lowest electrolysis potential and this result was consistent with the trend in the OER activity, as shown in Fig. 7. It is postulated that the addition of $Mg(OH)_2$ not only reduces the overpotential of the oxygen evolution reactions, but $Mg(OH)_2$ also has high catalytic activity.

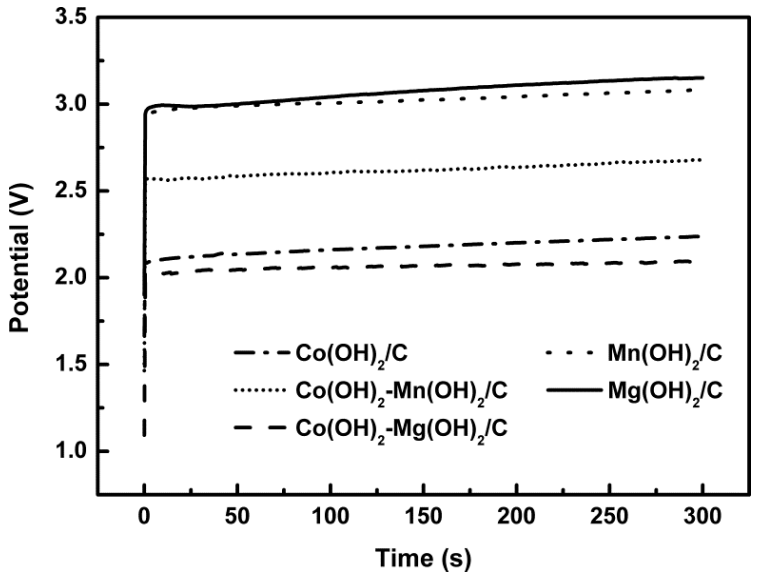

Figure 8. Comparison of performance of alkaline water electrolysis cells employing single metal hydroxide and bimetallic hydroxide catalysts as the anode in N_2-saturated 1 M KOH at scan rate of 20 mV/s; catalysts were prepared at pH 9.5. (Pt foil was used as the cathode).

Thus, it can be confirmed that the $Co(OH)_2$-$Mg(OH)_2$/C catalyst exhibits very high catalytic activity compared to the previously reported catalysts for the oxygen evolution reactions in alkaline water electrolysis.

4. CONCLUSION

In this study, carbon-supported $Co(OH)_2$ and $Mg(OH)_2$ mixed binary hydroxide catalysts were fabricated via a modified polyol method and were applied to the OER under alkaline conditions. Although the carbon-supported magnesium hydroxide catalyst, $Mg(OH)_2$/C, exhibits very low catalytic activity for the OER, surprisingly high OER activities in alkaline solutions could be achieved by mixing $Mg(OH)_2$ with $Co(OH)_2$/C compared with that achieved with other metal (Ni, Mn) catalysts. The optimal catalyst activity and the lowest overpotential was achieved when the ratio of $Co(OH)_2$ to $Mg(OH)_2$ in the $Co(OH)_2$-$Mg(OH)_2$/C catalyst was 84:16 for the sample prepared at pH 9.5. Thus, it is deduced that the carbon-supported $Mg(OH)_2$-$Co(OH)_2$/C catalyst reduces the overpotential and increases the overall reaction rate because the Co-OH bonding intermediate formed during the alkaline oxygen evolution reaction can be weakened by the presence of magnesium hydroxide.

ACKNOWLEDGEMENT
This work was supported by the New & Renewable Energy Core Technology Program of the Korea Institute of Energy Technology Evaluation and Planning (KETEP) with financing from the Ministry of Trade, Industry & Energy (No. 20133030011320), Republic of Korea. This work was supported by the INHA UNIVERSITY Research Grant.

References

1. M. S. Dresselhaus, I. L. Thomas, *Nature*, 414 (2001) 332.

2. M. Grätzel, *Nature*, 414 (2001) 338.
3. M. Lefèvre, E. Proietti, F. Jaouen, J. P. Dodelet, *Science*, 324 (2009) 71.
4. 4 H. A. Gasteiger, N. M. Marković, *Science*, 324 (2009) 48.
5. A. Döner, R. Solmaz, G. Kardaş, *Int. J. Hydrogen Energy*, 36 (2011) 7391.
6. P. Millet, R. Ngameni, S. A. Grigoriev, N. Mbemba, F. Brisset, A. Ranjbari, C. Etievant, *Int. J. Hydrogen Energy*, 35 (2010) 5043.
7. A. S. Arico, S. Siracusano, N. Briguglio, V. Baglio, A. Di Blasi, V. Antonucci, *J. Appl. Electrochem.*, 43 (2013) 107.
8. M. K. Hansen, D. Aili, E. Christensen, C. Pan, S. Eriksen, J. O. Jensen, J. H. Barner, Q. Li, N. J. Bjerrum, *Int. J. Hydrogen Energy*, 37 (2012) 10992.
9. E. Laouini, M. Hamdani, M.I.S. Pereira, J. Douch, M.H. Mendonca, Y. Berghoute, R.N. Singh, *Int. J. Hydrogen Energy*, 33 (2008) 4936.
10. B. Yeo, A. T. Bell, *J. Am. Chem. Soc.*, 133 (2011) 5587.
11. J. B. Gerken, J. G. MacAlpin, J. Y. Chen, M. K. Rigsby, W. H. Casey, R. D. Britt, S. S. Stahl, *J. Am. Chem. Soc.*, 133 (2011) 14431.
12. Y. Surendranath, M. Dinca, D. G. Nocera, *J. Am. Chem. Soc.*, 131 (2009) 2615.
13. J. J. Stracke, T. G. Finke, *J. Am. Chem. Soc.*, 133 (2011), 14872.
14. G. Y. Chen, S. R. Bare, T. E. *J. Electrochem. Soc.*, 149 (2002) A1092.
15. D.P. Lapham, A.C.C. Tseung, *J. Mater. Sci.*, 39, (2004) 251.
16. J. Masa, A. Zhao, W. Xia, M. Muhler, W. Schuhmann, *Electrochim. Acta*, 128 (2014) 271.
17. N. Garg, M. Mishara, Govind, A. K. Ganguli, *RSC Adv.*, 5 (2015) 84988.
18. L.M. Da Silva, L.A. De Faria, J.F.C. Boodts, *J. Electroanal. Chem.*, 532 (2002) 141.
19. I. Serebrennikova, V.I. Birss, *J. Mater. Sci.*, 36 (2001) 4331.
20. C. Bo, J.-Bao Li, J.-Hui Dai, *Mater. Lett.*, 58 (2004) 1415.
21. H. Guan, C. Shao, Y. Liu, N. Yu, X. Yang, *Solid State Commun.*, 131 (2004) 107.
22. Y. Jiang, Y. Wu, B. Xie, Y. Qian, *Mater. Chem. Phys.*, 74 (2002) 23.
23. E.B. Castro. S.G. Real, L.F.P. Dick, *Inter. J. Hydrogen Energy*, 29 (2004) 255.
24. G. Wu, N. Li, D.-Rui Zhou, K. Mitsuo, B.-Qing Xu, *J. Solid State Chem.*, 177 (2004) 3682.
25. M. Abbas, M. N. Islam, B. P. Rao, T. Ogawa, M. Takahashi, C. Kim, *Mater. Lett.*, 91 (2013) 326.
26. Z. Li, J. Yang, G. Xu, S. Wang, *J. Power Sources*, 242 (2013) 157.
27. S. Yuan, H. Lu, Z. Sun, L. Fan, X. Zhu, W. Zhang, *J. Electrochem. Soc.*, 163 (2016) A1181.
28. Z. Chang, Y. Yang, X. Wang, M. Li, Z. Fu, Y. Wu, R. Holze, *Sci. Rep.*, 5 (2015) 11931.
29. C. Feldmann, *Adv. Funct. Mater.*, 13 (2003) 101.
30. Z. Zhou, S. Wang, W. Zhou, G. Wang, L. Jiang, W. Li, S. Song, J. Liu, G. Sun, Q. Xin, *Chem. Commun.*, 3 (2003) 394.
31. H.S. Oh, J.G. Oh, Y.G. Hong, H.S. Kim, *Electrochim. Acta*, 52, (2007) 7278.
32. G.A. El-Shobaky, F.H.A Abdalla, A.M. Ghozza, *Thermochimica Acta*, 292 (1997), 123.
33. M. Rutkowska, Z. Piwowarska, E. Micek, L. Chmielarz, *Micropor. Mesopor. Mat.*, 209 (2015), 54.
34. T. Kessler, W.E. Triaca, A.J. Arvia, *J. Appl. Electrochem.*, 24, (1994), 310.
35. R. Subbaranman, D. Tripkovic, K.C. Chang, D. Strmcnik, A.P. Paulikas, P. Hirunsit, M. Chan, J. Greeley, V. Stamenkovic, N.M. Markovic, *Nature Mater.*, 11 (2012) 550.
36. I.M. Sadiek, A.M. Mohammad, M.E.E. Shakre, M.S.E. Deab, B.E.E. Anadouli, *J. Solid State Electrochem.*, 17 (2013) 871.
37. I.M. Sadiek, A.M. Mohammad, M.E.E. Shakre, M.S.E. Deab, *Int. J. Hydrogen Energy*, 37 (2012), 68.